BULLETIN OF THE POLISH ACADEMY OF SCIENCES
TECHNICAL SCIENCES, Vol. 73(1), 2025, Article number: e151958
DOI: 10.24425/bpasts.2024.151958

Identification and classification of turn short-circuit and demagnetization failures in PMSM using LSTM and GRU methods

Timur LALE* **and Gökhan YÜKSEK**

Department of Electrical and Electronics Engineering, Faculty of Architecture and Engineering, Batman University, Bati Raman Campus 72000, Batman, Turkey

Abstract. In an extremely broad range of industrial applications, especially in electric vehicles, permanent magnet synchronous motors (PMSMs) play a vital role. Any failure in PMSMs may cause possible safety hazards, a drop in productivity, and expensive downtime. Therefore, their reliable operation is essential. Accurate failure identification and classification allow for addressing problems before they escalate, which helps ensure the seamless operation of PMSMs and reduces the likelihood of equipment failure. Therefore, in this paper, novel failure identification methods based on gated recurrent unit (GRU) and long short-term memory (LSTM) from recurrent neural network (RNN) methods are proposed for early identification of stator inter-turn short circuit failure (ISCF) and demagnetization failure (DF) occurring in PMSMs under multiple operating conditions. The proposed methods use three-phase current signals recorded from the experimental study under multiple operating conditions of the motor as input data. In the proposed methods, both feature extraction and classification are executed within a unified framework. The experimental outcomes obtained demonstrate that the proposed methods can identify a total of six unique motor conditions, including three ISCF variations and two DF variations, with high accuracy. The LSTM and GRU approaches predicted the identification of failures with 98.23% and 98.72% accuracy, respectively. Compared to existing methods, the success of the proposed approaches is satisfactory. In addition, LSTM and GRU-based failure identification methods are also compared in detail for accuracy, precision, sensitivity, specificity, and training time in this study.

Keywords: gated recurrent unit; long short-term memory; fault diagnosis; PMSM.

1. INTRODUCTION

Electric vehicles (EVs) are of immense importance for a sustainable future and environmental protection. Carbon emissions and air pollution caused by traditional fossil-fuelled vehicles cause serious environmental problems worldwide. EVs minimize these problems thanks to their zero-emission operation. In addition, EVs, which attract attention with their energy efficiency and low operating costs, increase energy security by reducing dependence on fossil fuels. In this context, permanent magnet synchronous motor (PMSM) technology used in electric vehicles maximizes vehicle performance and energy savings by offering high efficiency and power density. PMSMs also stand out as the ideal power transmission system for electric vehicles with their low noise levels and long-lasting structures. As EVs become more widely adopted, the role of PMSMs in these vehicles becomes increasingly important. Advanced failure identification systems in PMSMs ensure early identification and resolution of potential issues, contributing to the reliability and efficiency of EVs. This capability not only enhances driver confidence but also supports the broader acceptance of EVs as a dependable mode of transportation [1]. PMSMs are widely used as basic electrical machines in renewable energy production, railway systems, and many other industries, apart from electric vehicles, due to their precise torque control, high-speed operation, and high power density [2]. Several failures in electric motors may arise despite continuous monitoring of the motor. Failures in PMSMs can result in reduced motor efficiency and associated system performance, reduced industrial production and potential safety hazards. Therefore, it is essential to diagnose or monitor the condition of PMSMs. The main components of the PMSM, the stator and rotor, specify the reliability and performance of the whole motor associated system. Inter-turn short-circuits failure (ISCF), and permanent magnet (PM) demagnetization failure (DF) are prevalent serious failures in the stator windings and rotor of PMSMs, respectively. These failures are mainly because of manufacturing deficiencies as well as thermal, mechanical, electrical and other environmental influences [3].

The rotor irreversible demagnetization is a severe problem that distorts the motor properties and reduces the output torque of PMSMs. The main reason for this failure is the condition related to its operation. The electric current generates a reverse magnetic field that resists the residual induction of the permanent magnets in the normal operation of the PMSMs. Because of this repeated operating condition, permanent magnets can undergo either partial demagnetization, affecting only part of the pole, or uniform demagnetization, affecting the entire pole.

*e-mail: timur.lale@batman.edu.tr

Manuscript submitted 2024-07-23, revised 2024-09-07, initially accepted for publication 2024-09-13, published in January 2025.

The permanent magnet can also be demagnetized by high temperatures [4]. Turn short-circuits commonly happen because of damage to the stator winding insulation, which is caused by electrical, thermal, and severe mechanical stresses that motors endure during operation, typically in challenging environmental conditions. Other factors that may speed up the deterioration of the stator winding insulation and lead to a short circuit include chemicals that could quicken the ageing of the insulation, field weakening, operation at loads over the rated values and high voltage oscillations of the inverters driving the motors [5]. The ISCF results in a high-amplitude current flowing through short circuit turns, causing local overheating of the stator winding, which can potentially cause significant damage to the motor and require it to be removed from service [6]. In order to prevent unforeseen downtimes in processes involving these motors due to operational interruptions, it is vital to consistently monitor the condition of the stator winding and identify and classify any damage at the earliest opportunity [5]. Early identification of failures allows for the appropriate scheduling of motor maintenance, resulting in lower repair expenses, reduced delays, and minimized production losses. Furthermore, it is crucial for sustainability and environmental issues because it decreases the creation of extra waste.

Given the previously noted risks from insufficient implementation of diagnostic methods and the increasing prevalence of PMSMs, it appears essential to diagnose their faults. In recent years, both university researchers and industry professionals have shown significant interest in it. To fulfil these demands, the improvement of such methods forces us to search for innovative solutions and the possibility of using the latest technologies. Choosing and using suitable artificial intelligence (AI) methods and signal processing techniques can enable the creation of fully automated systems for real-time motor condition monitoring.

There are two primary approaches for identifying and classifying motor failures: the traditional method and the AI-based technique. Traditional methods use signal processing algorithms. Wavelet transform (WT), discrete wavelet transform (DWT) [7], fast Fourier transform (FFT) [8], higher-order transforms, and Hilbert-Huang transform (HHF) [9] are some of these methods. Traditional methods use signals such as axial flux, torque, vibration, current, and voltage obtained from the motor as input variables to extract failure symptoms that can be used in failure identification. The most commonly used of these signals are the stator three-phase currents [10]. Harmonics of the phase current spectrum, only third harmonic [11], fifth and seventh harmonics [12] and only ninth harmonic [9] were used as ISCF identification indicators. In [13], it was proposed that the frequency band detail coefficients obtained by applying DWT to stator phase currents can be employed in turn short-circuit failure identification. Manala *et al.* [14] suggested the failure indicator derived from the reactive power excess for turn failure identification. In [8], the second and fourth harmonic components of the torque were proposed as ISCF symptoms for ISCF identification. HHT [15], DWT, and CWT [16] methods were proposed for the identification of demagnetization failure in PMSM. Delgado *et al.* [17] proposed the Vold-Kalman filter for the identification of partial demagnetization failure in PMSM. Mustafa *et al.* [18] investigated the effect of demagnetization failure on PMSM by finite element technique. Eker and Özsoy [19] investigated the effects of demagnetization failure on PMSM performance and efficiency. Ko *et al.* [20] proposed the eighth harmonic of the stator current as the fault indicator for the detection of demagnetization failure in PMSM. However, these traditional fault identification methods have several constraints. The computational complexity of both Fourier and wavelet transforms is notably high, significantly constraining their practical use in real-time signal processing. In addition, the Fourier transform, and matched filters are more appropriate for failure identification when systems operate under steady-state conditions. However, in real-life applications of industrial machines, including PMSMs, they often operate under transient or dynamic state conditions. Failures can also occur during non-steady states, requiring diagnostic methods that are applicable and versatile enough to identify failures over a variety of operating conditions. These obstacles highlight the significance of investigating AI-driven failure identification techniques that can overcome the shortcomings of traditional methods while also performing well under dynamic, real-time, and various operating conditions [21, 22].

The AI-driven approaches extract and analyze information from past fault data [23–25]. AI-based failure identification methods use signal processing algorithms and machine learning approaches in a hybrid manner [26]. Signal processing algorithms are applied to motor signals to obtain failure features. These features are then used as input data in machine learning methods to identify and classify the failure. Pietrzak and Wolkiewics [27] proposed a hybrid approach combining continuous wavelet transform (CWT) and convolutional neural networks (CNNs) for the identification of turn short-circuit failure. In the proposed approach, scalogram images obtained by applying CWT to current signals were employed as the input data of CNN. In [28], the second and fourth harmonic components of the torque obtained from the FFT analysis of the torque signal were used as input data in support vector machines (SVM), artificial neural networks (ANNs), k-nearest neighbour (KNN) methods to identify and classify the turn short circuit failure. Skowron [29] proposed the transfer learning method for inter-turn fault identification in PMSM. Haddad *et al.* [30] proposed the AdaBoost method based on vibration and vibration-current data combination for stator fault diagnosis in PMSM. In the proposed method, the use of features based on vibration and current data combination achieved more successful fault prediction results than the use of features based only on vibration. Shih *et al.* [31] suggested SVM and data-driven CNN approaches for the identification of ISCF in PMSM. But the proposed methods were implemented for one speed and two load cases and the low severity of ISCF identified in the study was 5%. In [32], a gradient boosting classifier was proposed for the identification of turn short circuit failure in PMSM. Statistical features obtained from current and vibration signals were employed as input features of the suggested classifier and the study was performed for a single speed condition. The turn short-circuit failure identification success of the proposed method was 95%. In [33], the one-dimensional local binary patterns (1D-LBP) approach was

suggested for feature extraction from current and voltage signals for identification of turn short-circuit failure in PMSM. The features obtained from 1D-LBP were used in the KNN algorithm and the turn failure identification success was 90%. While this approach can identify turn short-circuits across various operating conditions, the generated histogram cannot differentiate between distinct fault types. Lee *et al.* [34] proposed a recurrent neural networks (RNNs) approach for the identification of turn short-circuit failure in PMSM. Motor speed and three-phase current were employed as input data for the suggested method. However, the study was fulfilled for two different operating speeds. Kao *et al.* [35] suggested a hybrid approach combining wavelet packet transform (WPT) and 1D-CNN for the identification of bearing and demagnetization failures in PMSM. In the proposed approach, WPT was used for feature extraction from three-phase current and CNN was used as a classifier. In [36], the CNN method was proposed for the identification of demagnetization failure in PMSM. The input data of the CNN classifier was the images obtained by applying CWT to three-phase current signals. The lowest level of demagnetization failure identified in the proposed approach was 12.5%. Youn *et al.* [37] proposed a hybrid approach combining FFT and SVM for the identification of turn short-circuit and demagnetization failures in PMSM. The FFT was applied to the three-phase back electromotive force voltages and the fault harmonics obtained were used as the input data of the SVM classifier for failure identification. However, the proposed approach was applied for two different speed cases.

Although existing studies on fault diagnosis with deep learning and classical machine learning methods achieved significant success, works on early failure identification under multiple operating conditions of the motor remain limited. Another shortcoming of the existing methods is that they are used for the detection of uniform faults. An important scientific challenge in the field of diagnostics research is to develop methods that could identify failures at an early stage. In light of these constraints, this paper suggests innovative fault diagnosis models specifically crafted to tackle and alleviate these bottlenecks, marking a significant advancement towards more efficient and resilient PMSM failure identification methods. The LSTM and GRU models were used to diagnose faults in induction [38–42] and brushless DC motors [43]. However, LSTM and GRU methods were not utilized to identify demagnetization and inter-turn short-circuit failures in PMSMs, distinguishing the type of failure, and determining the severity of the failure. Therefore, novel identification of fault methods based on the developed LSTM and GRU are proposed for early detection of ISCFs and DFs in PMSM under different operating conditions. The following outlines the contribution of this paper:

- This paper seeks to enhance the dependability and sustainability of industrial processes by emphasizing the potential of innovative GRU and LSTM models for effective identification and classification of failures in PMSM.
- The proposed failure identification methods were performed for six different fault states, including three different ISCF states (2%, 12.5%, 25%) and two different DF (5%, 10%) states and under different operating conditions of the motor (eight various speed states and six various loading states).
- With the proposed novel fault detection methods based on LSTM and GRU, it is possible to effectively detect ISCFs (2%) and DFs (5%) in PMSM at the initial stage, classify the fault type and determine the fault severity with high accuracy.
- By reducing repair expenses and extending equipment lifespan, the proposed efficiency and accuracy of the model can offer cost savings for industries.

The flowchart of the failure identification approaches offered in this paper is given in Fig. 1.

2. EXPERIMENTAL SETUP AND DATA ACQUISITION

For diagnosing purposes, the ISCF and DF occurring in the PMSM, a total of five identical motors, three motors with 2%, 12.5%, 25% ISCF, and two motors with 5% and 10% DF, were manufactured at the FEMSAN electric motor factory. The turn fault was created in the motor single phase. There are 280 turns

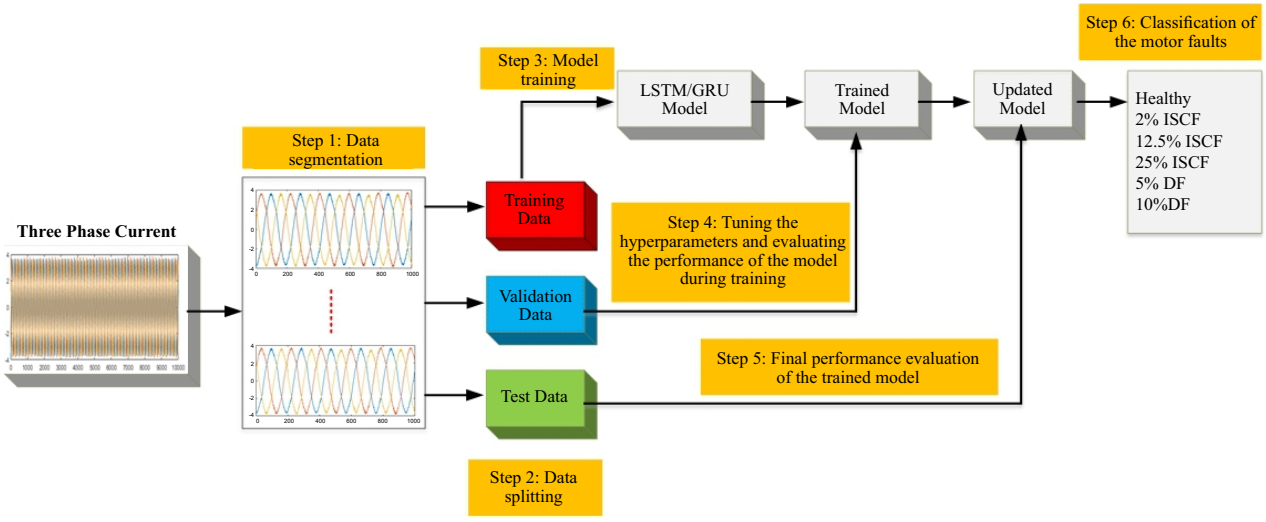

Fig. 1. Overview of the proposed methods

in each phase of the motors. Six turns for 2% ISCF, 35 turns for 12.5% ISCF and 70 turns for 25% ISCF are short-circuited. Through terminal connection, the motors were used for both healthy and faulty conditions. In the factory environment, motors with 5% and 10% demagnetization faults were produced. To create this fault in a controlled manner, the permanent magnets in the rotor were baked at high temperatures for a certain period, resulting in a deliberate weakening of the magnetic properties of the magnets. Thus, the magnetic field strength of the magnets was reduced at the desired rate. While ISCF motors were manufactured to operate in both healthy and faulty states, DF motors were manufactured to operate only in faulty states. Table 1 lists the properties of the PMSMs employed in the experimental investigation.

Table 1
Parameters of the motors utilized in the experimental kit

Rated torque	3 Nm
Number of turns/per phase	280
Rated power	1 kW
Phase winding resistance	7.6 Ω
Coil inductance	7.16 mH
Number of poles	8
Maximum speed	3000 rpm
Inertia torque	0.0001854 kgm

The experimental setup consists of a voltage source inverter drive, a DC eddy current brake, a data acquisition board, a torque meter, and voltage and current sensors (see Fig. 2). The DC eddy current brake was utilized to load the motor at the required ratios. The eddy brake and the tested motor were effectively integrated to minimize the impact of vibration on the motor signals. To operate the motor at the desired rotational speed, the FEMSAN servo driver unit was utilized. With the NI 6341-USB DAQ data acquisition card, information from current, voltage, and moment sensors is collected and transferred to the computer. The DAQ card has eight analogue inputs and two analogue outputs. In the experimental set, seven analogue inputs of the DAQ card were used, three inputs for three-phase current, three inputs for three-phase voltage, and one input for moment data. The data collected by the DAQ card was recorded with its analogue output in the interface program written in LabVIEW on the computer. With the experimental setup, the current, voltage, and torque signals of the motor were recorded at the desired speed and loading. The motor data were measured at a 10 kHz sampling frequency through sensors connected to the DAQ board and recorded to the computer using the LABVIEW software.

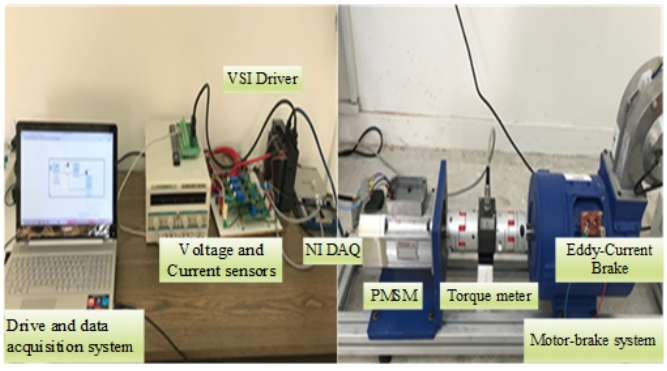

Fig. 2. Experimental setup

For each PMSM, three-phase current data was acquired at 0%, 25%, 50%, 75%, 100%, and 110% load and 800, 1000, 1200, 1400, 1600, 1800, 2000, and 2200 rpm. Three-phase current data was collected under 48 different scenarios, comprising six varying load states and eight distinct speed states. For motors with ISCF, the current data was recorded for 48 different cases for both healthy and faulty conditions, whereas for motors with DF, current data was recorded for 48 different cases only for the faulty condition. Three-phase current data were recorded for 1 s at a sampling frequency of 10 kHz for each case. The number of data points of the current recorded for each case is 10 000. Table 2 shows the number of samples of motor signals recorded in the healthy, ISCF and DF states of the PMSM.

Since deep learning methods work with large data sets, the current data recorded for each state was segmented and 0.1 s segments were created (see Fig. 3). This means that the number of data points in each segment will be 1000. The total number of samples for a case of three-phase current data obtained from the motor increases from 48 to 480. Since the signals of three different short-circuit faulty PMSMs are recorded in both faulty and healthy states, the total number of samples of the PMSM in a healthy state is $3 \times 480 = 1440$. The total number of samples for each of the 2% ISCF, 12.5% ISCF, 25% ISCF, 5% DF, and 10% DF cases is 480. The total number of samples of three-phase current data of PMSM for each case is given in Table 3. After randomly mixing the data set in the MATLAB environment, 30% of the data set was utilized as test data, 10% as validation data, and 60% as training data.

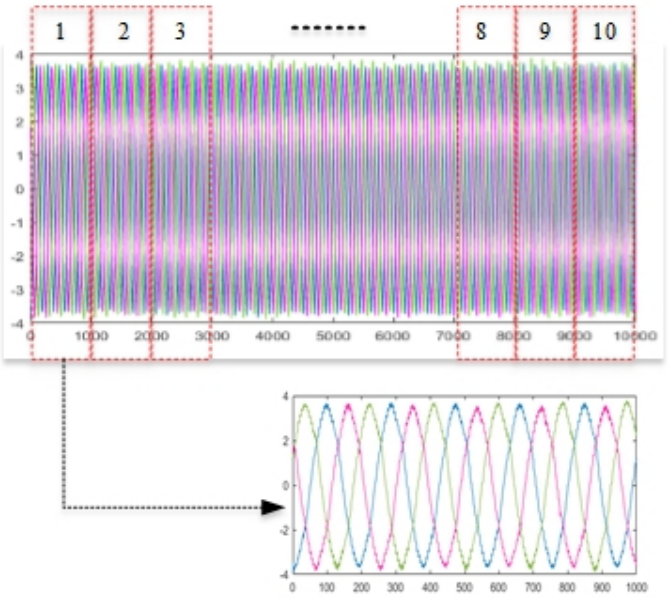

Fig. 3. Three-phase current segmentation

Table 2
Number of samples recorded from each motor

2% ISCF PMSM		12.5% ISCF PMSM		25% ISCF PMSM		5% DF PMSM	10% DF PMSM	Total number of samples
Healthy	Faulty	Healthy	Faulty	Healthy	Faulty	Faulty	Faulty	–
48	48	48	48	48	48	48	48	384

Table 3
Number of samples for each class of the three-phase current dataset

Classes	Healthy	%2 ISCF	%12.5 ISCF	%25 ISCF	%5 DF	%10 DF	Total samples
Number of samples	1440	480	480	480	480	480	3840

3. DEEP LEARNING METHODS FOR FAULT DETECTION

Deep learning, which uses multi-layer neural networks, is a branch of machine learning (hence the term "deep"). These networks excel at extracting intricate patterns from vast datasets, rendering them suitable for tasks such as speech recognition and image, as well as natural language processing, and, more recently, fault detection in motors [44]. The use of deep learning in motor fault detection represents a significant advancement over traditional methods. Using the capabilities of neural networks to analyze complex data, industries can achieve more reliable and efficient maintenance processes, ultimately leading to increased productivity and reduced operational costs [39]. However, successful implementation requires careful consideration of data acquisition, model selection, and computational resources. In this paper, novel GRU and LSTM approaches are used for the identification of failures and diagnosis of failure type and severity in PMSM.

3.1. Long short-term memory (LSTM)

LSTM, a variant of recurrent neural networks (RNN), finds extensive application in handling sequential data, such as time series or natural language. LSTMs were introduced to manage the issue of vanishing/exploding gradients that traditional RNNs suffer from when dealing with long-term dependencies. The key to LSTMs is their unique cell state and gating mechanism [39]. An LSTM cell comprises a cell state and three types of gates: a forget gate (f_t) an input gate (i_t), and an output gate (o_t), as shown in Fig. 4. The movement of information entering and exiting the cell state are controlled by these gates. The forget gate decides which information from the earlier cell state should be retained or eliminated. From the present input and prior concealed condition, fresh data to be preserved in the existing cell' status is regulated by the entry portal. How much of the current cell state is used for the final output is determined by the output gate. This gating mechanism enables LSTMs to choose what information to retain or discard across lengthy sequences, helping to address the vanishing gradient problem. The cell state acts like a conveyor belt, transferring relevant information across the entire sequence chain. LSTMs are able to effectively capture long-range dependencies, which traditional RNNs struggle with it [43, 45, 46].

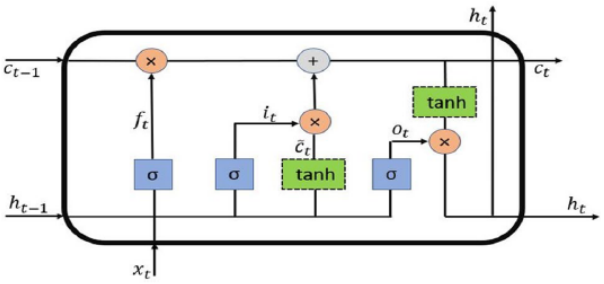

Fig. 4. The LSTM basic structure

LSTMs proved to be highly effective for various sequential data modelling tasks, such as time series forecasting, speech recognition, machine translation, and natural language processing. They have become a staple component in many state-of-the-art deep learning architectures for handling sequential data. In recent years, the LSTM model was widely utilized in failure identification of induction [38–42] and brushless DC motors [43, 47], and achieved successful results.

3.2. Gated recurrent unit (GRU)

GRUs are an alternative kind of gated RNN, introduced as a simpler alternative to LSTMs. Like LSTMs, GRUs are developed to solve the disappearing gradient issue of traditional RNNs when dealing with long sequences. The key components of a GRU are the candidate hidden state, the update gate, and the reset gate, as shown in Fig. 5. The reset gate dictates the extent to which the previous memory is erased and refreshed based on the new input. The update gate regulates the extent to which in-

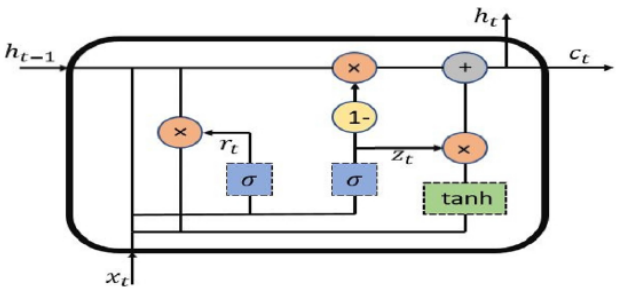

Fig. 5. The GRU basic structure

formation from both the preceding hidden state and the current input contributes to the calculation of the new hidden state [45]. Specifically, the GRU merges the forget and input gates found in LSTM into a unified update gate. It combines the cell state and hidden state vectors into a unified fully gated hidden state vector. This makes the GRU model simpler and more efficient than the LSTM. The reset gate allows the GRU to drop information from the previous hidden state, while the update gate determines how much of the new hidden state comes from the previous one. This gating mechanism helps GRUs better track long-range dependencies in subsequent data [48].

3.3. Design of LSTM and GRU for fault detection

In this paper, two different deep networks were developed and assessed as illustrated in Fig. 6. There are three recurring layers in the architecture of each of these models. The models offered are composed of Model 1 (a three-layer LSTM) and Model 2 (a three-layer GRU). Adding too many layers overcomplicates networks and can lead to overfitting. Thus, the study presented only a three-layer network. A fully connected layer with a softmax activation function is connected to the hidden layer in these designed models. The parameters used to train the designed GRU and LSTM models are given in Table 4. The same training parameters and the same architectural structures were employed to compare the classification success of the GRU and LSTM approaches. The classification layer computes the cross-entropy loss, which is then used in the optimization process to adjust the network weights. Adam is selected as the optimizer. The learning rate is set to 0.001.

Table 4
LSTM and GRU training options

Optimizer	Adam
Minibatch size	32
Validation frequency	497 iterations
Number of epochs	300
Learning rate	0.001

4. RESULTS AND DISCUSSION

The designed GRU and LSTM approaches were utilized to diagnose the type and severity of the failures. 30% of the dataset was employed for testing, 10% for validating, and 60% for training. The models were created in a MATLAB environment. The entire study was executed on a computer with an Intel® Core™ i7-6500U CPU @ 2.50 GHz and 16 GB of RAM. Accuracy and loss value graphs of the training progress of the proposed models are given in Fig. 7. Graphs of training accuracy and loss give insights into the model progression throughout the training period. A steady rise in the accuracy graph and a consistent drop in the loss graph during training suggest that the approach is undergoing stable training. During training, it is crucial for the gap between the validation and training accuracy curves to narrow, leading to their convergence. This indicates that the model is not overfitting and is generalizing effectively. Evidently, the models do not exhibit overfitting when analyzing the training progress graphs of LSTM and GRU in Fig. 7. In this way, it is possible to say that the models conduct the learning process over the training data set. The outcomes from the training progress of the GRU and LSTM approaches are introduced in Table 5. Table 5 shows that the GRU approach outperformed the LSTM approach in terms of training accuracy, loss value and training time.

Table 5
Results of training progression of LSTM and GRU models

	LSTM	GRU
Training accuracy	98.88%	100%
Training loss value	0.0523	0.0399
Validation accuracy	93.49%	94.79%
Validation loss value	0.2034	0.1401
Elapsed time	137 min 20 sec	85 min 12 sec

The trained GRU and LSTM approaches were evaluated for the diagnostic success of fault type and severity in PMSM using test data. The confusion matrix illustrating the classification

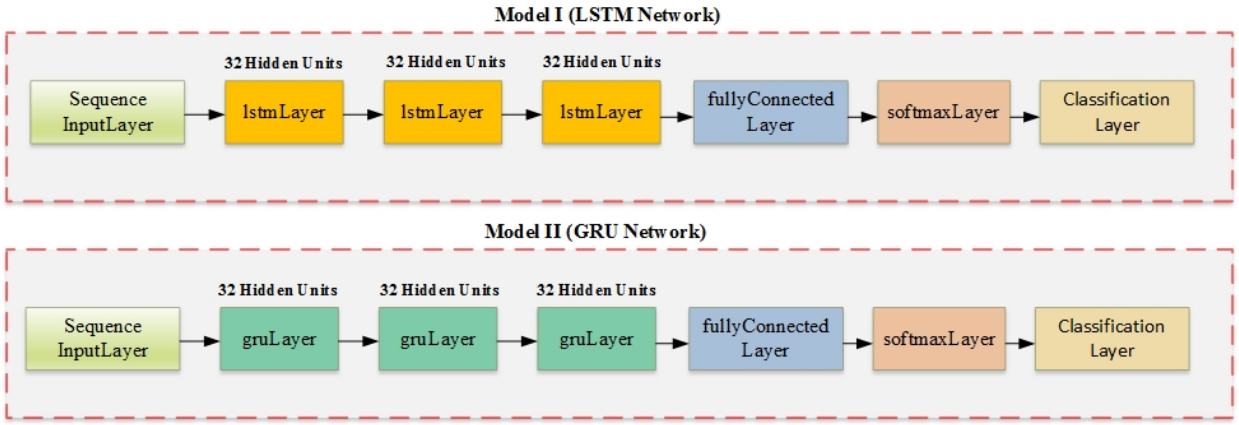

Fig. 6. LSTM and GRU models

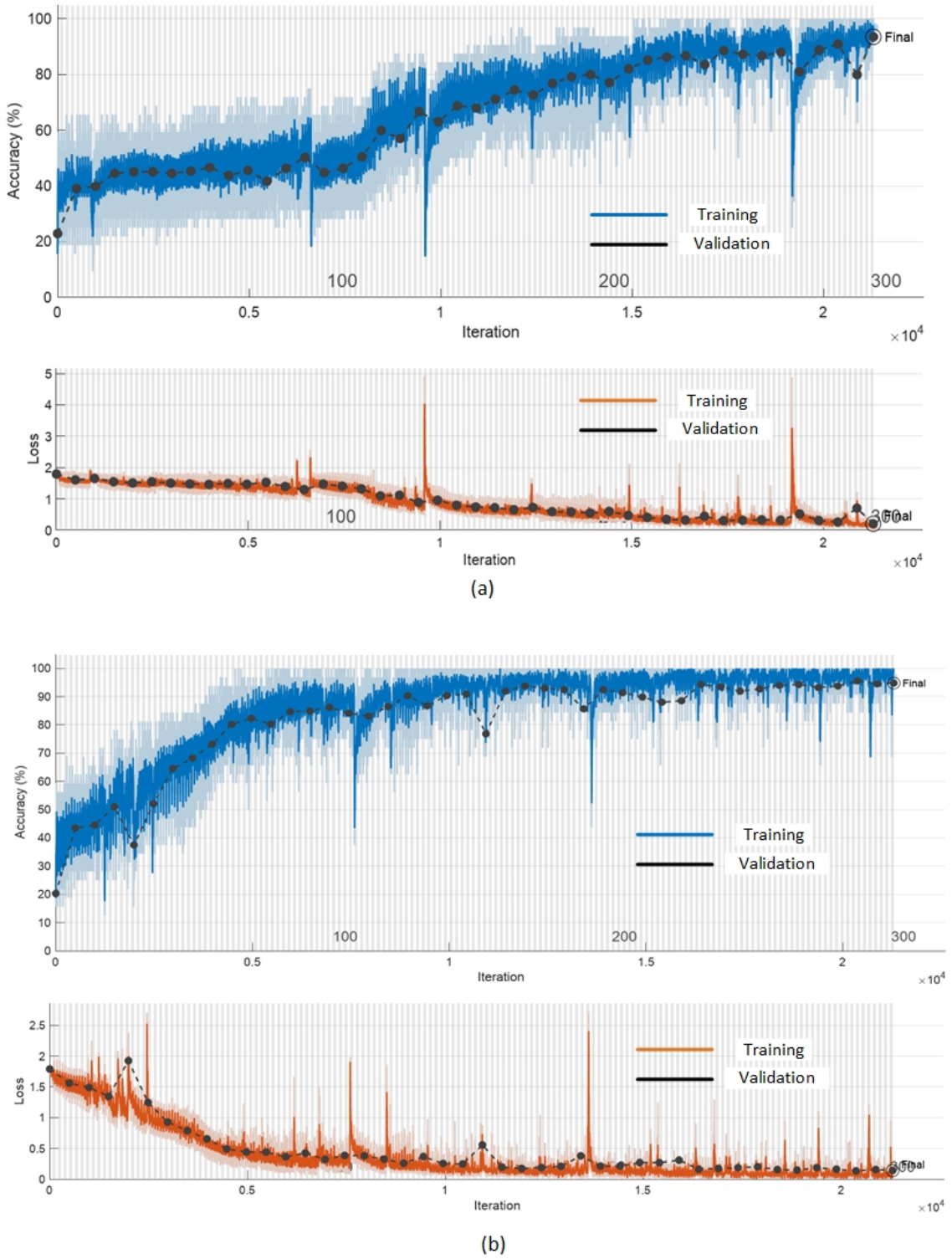

Fig. 7. (a) LSTM training progress, (b) GRU training progress

outcomes of the GRU and LSTM approaches for the motor test data is given in Fig. 8. In the confusion matrix, labels 0, 1, 2, 3, 4, and 5 correspond to healthy, 2% ISCF, 12.5% ISCF, 25% ISCF, 5% DF and 10% DF classes of the motor, respectively. Standard metrics are commonly used to assess a model performance in detail through confusion matrices. Based on the confusion matrix, these metrics rely on rates such as false positives (FP), true negatives (TN), true positives (TP), and false negatives (FN). Below are the corresponding formulas for each metric:

Precision measures the proportion of true positives among all positive estimates. It indicates how accurately the approach diagnoses positive instances [49]. The computation is illustrated

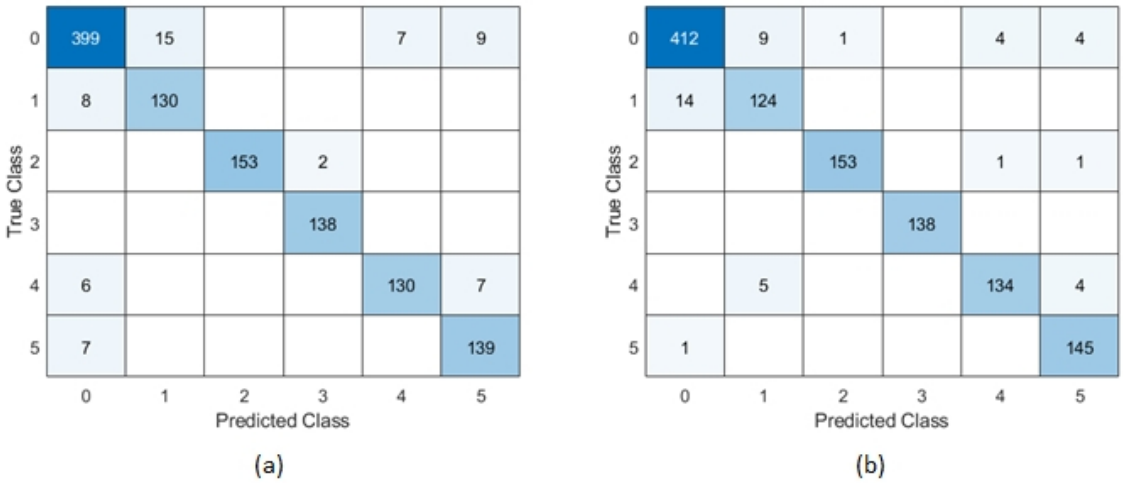

Fig. 8. (a) LSTM and (b) GRU confusion matrix

in equation (1)

$$\text{Precision} = \frac{TP}{TP+FP} \times 100. \tag{1}$$

Sensitivity represents the percentage of accurately identified observations within a specific class relative to the total number of observations in that class. It shows the ability of the classifier to accurately recognize data that genuinely pertains to the positive category [49]. The formula can be found in equation (2)

$$\text{Sensitivity} = \frac{TP}{TP+FP} \times 100. \tag{2}$$

Specificity measures the proportion of correctly predicted negative class data by the classifier [49]. The evaluation can be conducted using equation (3)

$$\text{Specificity} = \frac{TN}{TN+FP} \times 100. \tag{3}$$

F1-score stands as another frequently employed metric in evaluating model effectiveness. Equation (4) calculates this metric by combining precision and recall values through a weighted average [49]

$$F1\text{-score} = \frac{(\text{recall}) \times (\text{precision}) \times 2}{(\text{recall}) + (\text{precision})}. \tag{4}$$

Accuracy measures the proportion of accurately classified data within the model test set, calculated from the training data. This calculation is defined by equation (5) [49]

$$\text{Accuracy} = \frac{TP+TN}{TP+TN+FP+FN} \times 100. \tag{5}$$

Table 6 summarizes the performance metrics obtained from the distributions derived from the confusion matrices. As seen in Table 6, the LSTM and GRU models predicted the diagnosis of ISCF and DF in PMSM with an average accuracy of over

Table 6
Overall performance metrics of LSTM and GRU models

Class label	LSTM					GRU				
	Precision (%)	Sensitivity (%)	Specificity (%)	F1-score (%)	Accuracy (%)	Precision (%)	Sensitivity (%)	Specificity (%)	F1-score (%)	Accuracy (%)
0	95.00	92.79	97.08	93.88	95.48	96.49	95.81	97.92	96.15	97.13
1	89.66	94.20	98.52	91.87	98.00	89.86	89.86	98.62	89.86	97.57
2	100	98.71	100	99.35	99.83	99.35	98.71	99.90	99.03	99.74
3	98.57	100	99.80	99.28	99.83	100	100	100	100	100
4	94.89	90.91	99.30	92.86	98.26	96.40	93.71	99.50	95.04	98.78
5	89.68	95.21	98.41	92.36	98.00	94.16	99.32	99.10	96.67	99.13
Average accuracy	**94.63**	**95.30**	**98.85**	**94.93**	**98.23**	**96.04**	**96.23**	**99.17**	**96.12**	**98.72**

98%. In terms of specificity, sensitivity, precision, F1-score, and accuracy metrics, the GRU model performed better than the LSTM model.

4.1. Comparison of the findings from this paper with those reported in the existing literature

The comparison of the outcomes of the methods suggested in this paper with the works in the literature is given in Table 7. In Youn *et al.* [37], to detect DF and ISCF in PMSM and classify faults, fault-dependent varying harmonics were detected by applying FFT to back electromotive force (BEMF) voltages. Principal component analysis (PCA) was employed to convert the dimensions of the harmonics into two dimensions. Using the features obtained as a result of this process in the SVM algorithm, the classification of faults was predicted with an accuracy of 92.5% for 300 rpm and 97.5% for 500 rpm. However, the study was not evaluated for more than one speed state at the same time [37]. In [2], the classification of DF and ISCF was predicted with 97.5% accuracy using CNN hybrid with local feature extraction method with self-attention mechanism. However, the study did not consider the different severity of DF and ISCF. Yan and Hu [50], used a hybrid multi-scale residual dilated (MD)-CNN and bidirectional (Bi)-LSTM method for fault diagnosis in PMSM. The features obtained from the signals with the MD-CNN method were used in the BiLSTM algorithm for failure identification. Using three-phase current, vibration, and the fused of vibration and three-phase current signals, the fault diagnosis was predicted with 92.81%, 72.81%, and 98.63% accuracy, respectively. The lowest severities of ISCF and DF detected in the proposed study are 4.6% and 20%, respectively [50]. The fault classification accuracy rates of the LSTM and GRU methods proposed in this paper are 98.23% and 98.72%, respectively. Compared with similar studies in Table 7, the suggested GRU- and LSTM-based fault diagnosis performance is satisfactory. The algorithms of the suggested GRU- and LSTM-based fault diagnosis approaches are not complex compared to similar works in Table 7. In the suggested LSTM and GRU approaches, the process of extracting features and classifying them was conducted within a unified learning framework and only the raw three-phase current signal was used as the input signal.

5. CONCLUSIONS

In this study, novel LSTM- and GRU-based failure identification approaches are suggested for the identification and classification of turn and demagnetization failures in PMSMs under multiple operating conditions. The failure detection and failure type classification using LSTM and GRU methods were predicted with over 98% accuracy. The classification success of the proposed methods is satisfactory when compared with similar studies in the literature. It is possible to detect the turn failure and the demagnetization failure in the PMSM at the initial stage with the proposed methods. The lowest ISCF and DF severities detected in this study were 2% and 5%, respectively. When the LSTM and GRU methods were compared in terms of classification success, F1 score, precision, sensitivity, specificity, and training time, the GRU method performed better.

With the proposed methods of fault diagnosis, it will be possible to diagnose the faults that can occur in the PMSMs that are used in the industry at an early stage. In this way, stoppage of production in the industry, loss of time, and human injuries are prevented and continuity in production is ensured. The proposed new diagnostic methods can also prevent electric vehicles from staying on the road. The proposed diagnostic methods can be used in future studies to detect other faults, eccentricity, and bearing faults occurring in PMSM.

The application of the proposed methods to real systems in industrial and electric vehicle applications is possible by continuous monitoring of stator phase currents with current sensors integrated into the motors. These collected data are analyzed using the proposed deep learning algorithms and faults are detected automatically. Thus, potential failures in electric vehicles or industrial motor systems can be detected early, optimizing safety, efficiency, and maintenance costs.

REFERENCES

[1] Y. Jiang, B. Ji, J. Zhang, J. Yan, and W. Li, "An Overview of Diagnosis Methods of Stator Winding Inter-Turn Short Faults in Permanent-Magnet Synchronous Motors for Electric Vehicles," *World Electr. Veh. J.*, vol. 15, no. 4, p. 165, Apr. 2024, doi: 10.3390/wevj15040165.

[2] T. Peng, C. Ye, C. Yang, Z. Chen, K. Liang, and X. Fan, "A novel fault diagnosis method for early faults of PMSMs under multiple

Table 7
Comparison of the findings from this paper with those reported in the existing literature

Reference	Approach	Type of motor	Failure type	Feature	Accuracy (%)
Youn *et al.* [37]	FFT + PCA + SVM	PMSM	ISCF and DF	BEMF voltages (for 300 rpm) (for 500 rpm)	92.5 97.5
Peng *et al.* [2]	SaM + CNN	PMSM	ISCF and DF	Sensor signals & motor speed	97.5
Yan and Hu [50]	MD + CNN + BiLSTM	PMSM	ISCF and DF	Three-phase current Vibration Current & vibration	92.81 72.81 98.63
Proposed	LSTM GRU	PMSM	ISCF and DF	Three-phase current	98.23 98.72

operating conditions," *ISA Trans.*, vol. 130, pp. 463–476, 2022, doi: 10.1016/j.isatra.2022.04.023.

[3] L. Vancini, M. Mengoni, G. Rizzoli, L. Zarri, and A. Tani, "Local Demagnetization Detection in Six-Phase Permanent Magnet Synchronous Machines," *IEEE Trans. Ind. Electron.*, vol. 71, no. 6, pp. 5508–5518, Jun. 2024, doi: 10.1109/TIE.2023.3294603.

[4] J. Faiz, H. Nejadi-Koti, and Z. Valipour, "Comprehensive review on inter-turn fault indexes in permanent magnet motors," *IET Electr. Power Appl.*, vol. 11, no. 1, pp.142–156, 2017, doi: 10.1049/iet-epa.2016.0196.

[5] C. Zeng, S. Huang, J. Lei, Z. Wan, and Y. Yang, "Online Rotor Fault Diagnosis of Permanent Magnet Synchronous Motors Based on Stator Tooth Flux," *IEEE Trans. Ind. Appl.*, vol. 57, no. 3, pp. 2366–2377, May 2021, doi: 10.1109/TIA.2021.3058541.

[6] T. Orlowska-Kowalska *et al.*, "Fault Diagnosis and Fault-Tolerant Control of PMSM Drives–State of the Art and Future Challenges," *IEEE Access*, vol. 10, pp. 59979–60024, 2022, doi: 10.1109/ACCESS.2022.3180153.

[7] J. Fang, Y. Sun, Y. Wang, B. Wei, and J. Hang, "Improved ZSVC-based fault detection technique for incipient stage inter-turn fault in PMSM," *IET Electr. Power Appl.*, vol. 13, no. 12, pp. 2015–2026, Dec. 2019, doi: 10.1049/iet-epa.2019.0016.

[8] T. Lale and B. Gümüş, "A New Approach based on Electromechanical Torque for Detection of Inter-Turn Fault in Permanent Magnet Synchronous Motor," *Electr. Power Compon. Syst.*, vol. 49, no. 18–19, pp. 1499–1511, Nov. 2021, doi: 10.1080/15325008.2022.2133193.

[9] J. Urresty, J. Riba, L. Romeral, J. Rosero, and J. Serna, "Stator short circuits detection in PMSM by means of Hilbert-Huang transform and energy calculation," in *2009 IEEE International Symposium on Diagnostics for Electric Machines, Power Electronics and Drives*, 2009, vol. 5, no. 2, pp. 1–7, doi: 10.1109/DEMPED.2009.5292789.

[10] G. Niu, X. Dong, and Y. Chen, "Motor Fault Diagnostics Based on Current Signatures: A Review," *IEEE Trans. Instrum. Meas.*, vol. 72, pp. 1–19, 2023, doi: 10.1109/TIM.2023.3285999.

[11] F. Cira, M. Arkan, and B. Gumus, "Detection of Stator Winding Inter-Turn Short Circuit Faults in Permanent Magnet Synchronous Motors and Automatic Classification of Fault Severity via a Pattern Recognition System," *J. Electr. Eng. Technol.*, vol. 11, no. 2, pp. 416–424, Mar. 2016, doi: 10.5370/JEET.2016.11.2.416.

[12] J.-C. Urresty, J.-R. Riba, and L. Romeral, "Application of the zero-sequence voltage component to detect stator winding inter-turn faults in PMSMs," *Electr. Power Syst. Res.*, vol. 89, pp. 38–44, Aug. 2012, doi: 10.1016/j.epsr.2012.02.012.

[13] T. Lale, M.S. Ozerdem, and B. Gumus, "Analysis of Permanent Magnet Synchronous Motor Current in Healthy and Short Circuit Failure Cases with Discrete Wavelet Transform," in *2019 Innovations in Intelligent Systems and Applications Conference (ASYU)*, 2019, pp. 1–5, doi: 10.1109/ASYU48272.2019.8946330.

[14] S. Manala and J. Seshadrinath, "Reactive Power-Residual-Based Stator Interturn Fault Detection in PMSM Drive," *IEEE Trans. Ind. Appl.*, vol. 60, no. 3, pp. 4888–4898, 2024, doi: 10.1109/TIA.2024.3351627.

[15] J. Rosero, L. Romeral, J.A. Ortega, and J.C. Urresty, "Demagnetization fault detection by means of Hilbert Huang transform of the stator current decomposition in PMSM," in *2008 IEEE International Symposium on Industrial Electronics*, 2008, pp. 172–177, doi: 10.1109/ISIE.2008.4677217.

[16] J.C. Urresty, J.R. Riba, M. Delgado, and L. Romeral, "Detection of demagnetization faults in surface-mounted permanent magnet synchronous motors by means of the zero-sequence voltage component," *IEEE Trans. Energy Convers.*, vol. 27, no. 1, pp. 42–51, 2012, doi: 10.1109/TEC.2011.2176127.

[17] C. Wang, M. Delgado Prieto, L. Romeral, Z. Chen, F. Blaabjerg, and X. Liu, "Detection of Partial Demagnetization Fault in PMSMs Operating Under Nonstationary Conditions," *IEEE Trans. Magn.*, vol. 52, no. 7, pp. 1–4, Jul. 2016, doi: 10.1109/TMAG.2015.2511003.

[18] M. Eker and M. Özsoy, "Investigation of the effect of demagnetization fault at Line Start AF-PMSM with FEM," *Acad. Platf. J. Eng. Smart Syst.*, vol. 10, no. 2, pp. 94–100, May 2022, doi: 10.21541/apjess.1007894.

[19] M. Eker and M. Özsoy, "Effect of demagnetization faults on line start AF-PMSM performance," *J. Power Electron.*, vol. 22, no. 6, pp. 1001–1009, Jun. 2022, doi: 10.1007/s43236-022-00439-5.

[20] Y. Ko, Y. Lee, J. Oh, J. Park, H. Chang, and N. Kim, "Current signature identification and analysis for demagnetization fault diagnosis of permanent magnet synchronous motors," *Mech. Syst. Signal Process.*, vol. 214, no. April, p. 111377, 2024, doi: 10.1016/j.ymssp.2024.111377.

[21] S.M. Baba, I. Bala, G. Dhiman, A. Sharma, and W. Viriyasitavat, "Automated diabetic retinopathy severity grading using novel DR-ResNet + deep learning model," *Multimed. Tools Appl.*, vol. 83, no. 28, pp. 71789–71831, Feb. 2024, doi: 10.1007/s11042-024-18434-2.

[22] Pinki *et al.*, "Artificial intelligence-enabled smart city management using multi-objective optimization strategies," *Expert Syst.*, Mar. 2024, doi: 10.1111/exsy.13574.

[23] S.I. Evangeline, S. Darwin, and E. Fantin Irudaya Raj, "A deep residual neural network model for synchronous motor fault diagnostics," *Appl. Soft Comput.*, vol. 160, p. 111683, Jul. 2024, doi: 10.1016/j.asoc.2024.111683.

[24] N. Sehrawat, S. Vashisht, A. Singh, G. Dhiman, W. Viriyasitavat, and N.S. Alghamdi, "A power prediction approach for a solar-powered aerial vehicle enhanced by stacked machine learning technique," *Comput. Electr. Eng.*, vol. 115, p. 109128, Apr. 2024, doi: 10.1016/j.compeleceng.2024.109128.

[25] B. Gümüs, H. Kılıç, C. Haydaroglu, and U.Y. Butakın, "Fault Type and Fault Location Detection in Transmission Lines with 6-Convolutional Layered CNN," *Bull. Pol. Acad. Sci. Tech. Sci.*, p. e151047, Jul. 2024, doi: 10.24425/bpasts.2024.151047.

[26] A. Alferaidi *et al.*, "Node Multi-Attribute Network Community Healthcare Detection Based on Graphical Matrix Factorization," *J. Circ. Syst. Comput.*, vol. 33, no. 05, p. 2450080, Mar. 2024, doi: 10.1142/S0218126624500804.

[27] P. Pietrzak and M. Wolkiewicz, "Application of continuous wavelet transform and convolutional neural networks in fault diagnosis of PMSM stator windings," *Bull. Pol. Acad. Sci. Tech. Sci.*, p. e150202, Apr. 2024, doi: 10.24425/bpasts.2024.150202.

[28] T. Lale and B. Gümüş, "An effective torque-based method for automatic turn fault detection and turn fault severity classification in permanent magnet synchronous motor," *Electr. Eng.*, vol. 106, no. 3, pp. 2865–2876, Jun. 2024, doi: 10.1007/s00202-023-02113-w.

[29] M. Skowron, "Analysis of PMSM Short-Circuit Detection Systems Using Transfer Learning of Deep Convolutional Networks,"

Power Electron. Drives, vol. 9, no. 1, pp. 21–33, 2024, doi: 10.2478/pead-2024-0002.

[30] L.A. Al-Haddad, S.S. Shijer, A.A. Jaber, S.T. Al-Ani, A.A. Al-Zubaidi, and E.T. Abd, "Application of AdaBoost for stator fault diagnosis in three-phase permanent magnet synchronous motors based on vibration–current data fusion analysis," *Electr. Eng.*, vol. 106, no. 4, pp. 4527–4542, 2024, doi: 10.1007/s00202-023-02195-6.

[31] K.J. Shih, M.F. Hsieh, B.J. Chen, and S.F. Huang, "Machine Learning for Inter-Turn Short-Circuit Fault Diagnosis in Permanent Magnet Synchronous Motors," *IEEE Trans. Magn.*, vol. 58, no. 8, pp. 1–7, 2022, doi: 10.1109/TMAG.2022.3169173.

[32] L.A. Al-Haddad, A.A. Jaber, M.N. Hamzah, and M.A. Fayad, "Vibration-current data fusion and gradient boosting classifier for enhanced stator fault diagnosis in three-phase permanent magnet synchronous motors," *Electr. Eng.*, vol. 106, no. 3, pp. 3253–3268, Jun. 2024, doi: 10.1007/s00202-023-02148-z.

[33] M.R. Minaz, "An effective method for detection of stator fault in PMSM with 1D-LBP," *ISA Trans.*, vol. 106, pp. 283–292, 2020, doi: 10.1016/j.isatra.2020.07.013.

[34] H. Lee, H. Jeong, G. Koo, J. Ban, and S.W. Kim, "Attention Recurrent Neural Network-Based Severity Estimation Method for Interturn Short-Circuit Fault in Permanent Magnet Synchronous Machines," *IEEE Trans. Ind. Electron.*, vol. 68, no. 4, pp. 3445–3453, Apr. 2021, doi: 10.1109/TIE.2020.2978690.

[35] I.H. Kao, W.J. Wang, Y.H. Lai, and J.W. Perng, "Analysis of Permanent Magnet Synchronous Motor Fault Diagnosis Based on Learning," *IEEE Trans. Instrum. Meas.*, vol. 68, no. 2, pp. 310–324, 2019, doi: 10.1109/TIM.2018.2847800.

[36] M. Eker and B. Gündogan, "Demagnetization fault detection of permanent magnet synchronous motor with convolutional neural network," *Electr. Eng.*, vol. 105, no. 3, pp. 1695–1708, Jun. 2023, doi: 10.1007/s00202-023-01768-9.

[37] Y.W. Youn, D.H. Hwang, S.J. Song, and Y.H. Kim, "Detection and classification of demagnetization and short-circuited turns in permanent magnet synchronous motors," *J. Electr. Eng. Technol.*, vol. 13, no. 4, pp. 1613–1621, 2018, doi: 10.5370/JEET.2018.13.4.1614.

[38] M. Hussain *et al.*, "Stator winding fault detection and classification in three-phase induction motor," *Intell. Autom. Soft Comput.*, vol. 29, no. 3, pp. 869–883, 2021, doi: 10.32604/iasc.2021.017790.

[39] M. Hussain, T. Din Memon, I. Hussain, Z. Ahmed Memon, and D. Kumar, "Fault Detection and Identification Using Deep Learning Algorithms in Induction Motors," *Comput. Model. Eng. Sci.*, vol. 133, no. 2, pp. 435–470, 2022, doi: 10.32604/cmes.2022.020583.

[40] R.H. Kılıç and E. Dandıl, "Asenkron Motor Rulman Hatalarının Uzun – Kısa Süreli Bellek Tipi Derin Sinir Ağlarıile Otomatik SınıflandırılmasıAutomatic Classification of Induction Motor Bearing Faults using Long – Short Term Memory Deep Neural Networks," *Avrupa Bilim Ve Teknoloji Dergisi*, vol. 32, pp. 508–513, 2021, doi: 10.31590/ejosat.1039836 (in Turkish).

[41] D. Xiao, Y. Huang, C. Qin, H. Shi, and Y. Li, "Fault Diagnosis of Induction Motors Using Recurrence Quantification Analysis and LSTM with Weighted BN," *Shock Vib.*, vol. 2019, p. 8325218, 2019, doi: 10.1155/2019/8325218.

[42] J. Vanga *et al.*, "Fault classification of three phase induction motors using Bi-LSTM networks," *J. Electr. Syst. Inf. Technol.*, vol. 10, no. 1, p. 28, 2023, doi: 10.1186/s43067-023-00098-x.

[43] T. Zimnickas, J. Vanagas, K. Dambrauskas, A. Kalvaitis, and M. Ažubalis, "Application of advanced vibration monitoring systems and long short-term memory networks for brushless DC motor stator fault monitoring and classification," *Energies*, vol. 13, no. 4, p. 820, 2020, doi: 10.3390/en13040820.

[44] F. Husari and J. Seshadrinath, "Early Stator Fault Detection and Condition Identification in Induction Motor Using Novel Deep Network," *IEEE Trans. Artif. Intell.*, vol. 3, no. 5, pp. 809–818, 2022, doi: 10.1109/TAI.2021.3135799.

[45] A. Kumar, A. Parey, and P.K. Kankar, "A New Hybrid LSTM-GRU Model for Fault Diagnosis of Polymer Gears Using Vibration Signals," *J. Vib. Eng. Technol.*, vol. 12, no. 2, pp. 2729–2741, 2024, doi: 10.1007/s42417-023-01010-7.

[46] A. Sherstinsky, "Fundamentals of Recurrent Neural Network (RNN) and Long Short-Term Memory (LSTM) network," *Phys. D Nonlinear Phenom.*, vol. 404, p. 132306, 2020, doi: 10.1016/j.physd.2019.132306.

[47] P. Suawa, T. Meisel, M. Jongmanns, M. Huebner, and M. Reichenbach, "Modeling and Fault Detection of Brushless Direct Current Motor by Deep Learning Sensor Data Fusion," *Sensors*, vol. 22, no. 9, p. 3516, 2022, doi: 10.3390/s22093516.

[48] J.H. Lee and J.K. Hong, "Comparative Performance Analysis of RNN Techniques for Predicting Concatenated Normal and Abnormal Vibrations," *Electronics*, vol. 12, no. 23, p. 4778, 2023, doi: 10.3390/electronics12234778.

[49] M. Ertargin, O. Yildirim, and A. Orhan, "Mechanical and electrical faults detection in induction motor across multiple sensors with CNN-LSTM deep learning model," *Electr. Eng.*, 2024, doi: 10.1007/s00202-024-02420-w.

[50] G. Yan and Y. Hu, "Inter-turn short circuit and demagnetization fault diagnosis of ship PMSM based on multiscale residual dilated CNN and BiLSTM," *Meas. Sci. Technol.*, vol. 35, no. 4, p. 046105, Apr. 2024, doi: 10.1088/1361-6501/ad19c0.